International Institute of Welding

RUSSIAN DELEGATION
AMERICAN DELEGATION

IIW Document XIII-2004-04

PHYSICS AND MECHANISM OF ULTRASONIC IMPACT TREATMENT

Efim Statnikov
Applied Ultrasonics,
2900 Crestwood Blvd.,
Alabama, 35210,
USA
Northern Scientific and Technology Company (NSTC),
6 Voronin St.,
Severodvinsk, 164500,
Russia

ABSTRACT

It has been acknowledged that ultrasonic impact treatment (UIT) occupies a firm position among methods for improving the reliability of welded joints, particularly their fatigue strengths. Developed in Russia in the early 1970s, this process has aroused considerable interest among experts and researchers in the area of fatigue and fabrication of welded structures. This interest reflects the benefits of the treatment; the small dimensions, high power and ease-of-use of the tools; good control of the treatment parameters; consistency; economic feasibility and safety; the wide range of practical applications.

This paper presents technical aspects of the process, including an experimental and theoretical description of the physics and the means of controlling the ultrasonic impact parameters. In addition, the efficiency of ultrasonic as compared to single impacts, such as obtained with peening processes, is assessed. Finally, it describes the mechanism of the effect on materials, feedback mode, in-process control of the treatment quality, tools and power supplies designed on the basis of the results of investigations of UIT.

1. INTRODUCTION AND BACKGROUND

The ultrasonic impact treatment (UIT) method may conventionally be classed with techniques that directly deform the surface with the use of ultrasonic vibrations. The development of these methods dates back to 1950s and is associated with the efforts of I.I. Mukhanov [1], A.V. Mordvintseva [2] and others, which are characterized by employing continuous ultrasonic vibrations at the ultrasonic transducer output end strengthened with hard materials (carbide-containing alloys, artificial diamonds etc.) and being in direct contact with the treated surface. As a result, a relatively thin surface layer of the treated material was plastically deformed, producing modifications of the surface microrelief and redistribution of residual stresses in this layer.

Subsequently in 1960s, N.A. Krylov et al. introduced an intermediate mass in the form of a free ball between the output end of the ultrasonic transducer and the material being treated [3]. In this work, the method of oscillating system excitation replicated the continuous ultrasonic excitation used in the efforts referenced above. The treatment process was accompanied by random impacts of the intermediate mass at a frequency significantly lower than that of initiating ultrasonic vibrations. This engineering solution enhanced somewhat the intensity of the surface layer plastic deformation. However, an excess freedom of ball random displacements could not provide sufficient consistency of effects in depth.

In the early 1970s, E.Sh. Statnikov proposed a method of ultrasonic impact treatment [4], which is finding expanding applications in various industries, including manufacture and maintenance of welded structures and machinery components. This method differs fundamentally in that it employs free needle indenters as impacting elements that move along the axis of the oscillating system and have a normalized wavelength relative to the carrier ultrasonic frequency. The indenters are installed in separate guiding holes and excited by modulation pulses of the carrier resonance frequency of the ultrasonic oscillation system. This engineering solution provides high-intensity ultrasonic impacts accompanied by ultrasonic vibrations of indenters in a gap and together with the surface being treated. These impacts initiate highly effective plastic deformation and transfer therethrough high-intensity ultrasonic vibrations and ultrasonic stress waves into the material being treated. A combination of such factors of the ultrasonic impact creates necessary prerequisites to modify properties and conditions of the surface and sub-surface material at a specified depth.

Later on, G.I. Prokopenko et al. [5] replicated the engineering solution [4] with continuous excitation of the ultrasonic transducer. In terms of the impact frequency spectrum, the results obtained are close to those obtained from the ball used as the intermediate mass. In this case, the relation between the time of impact upon the treated surface and the ultrasonic transducer operation time varies randomly in the range from 0.0001 to 0.05.

Alternatively, the pulse excitation of ultrasonic impacts in accordance with the method [4] makes it possible to intentionally control the generation and parameters of impacts, to maintain the relation referenced above in the range from 0.1 to 0.3 and to constantly obtain the information about the process and treatment quality during pause between impulses/impacts based on the response of the oscillating system “tool-workpiece” via the striction feedback signal.

The development of the method [4] in the late 1990s and early 2000s [6-22] resulted in the ***Esonix*** technology that supported a firm position of the ultrasonic impact treatment among well-known techniques of improving fatigue resistance of welded structures, including surface plastic deformation methods.

2. EXPERIMENTAL VERIFICATION OF UIT TECHNOLOGICAL EFFECTIVENESS

The ***Esonix*** technology has aroused considerable interest due to its economical effectiveness, possible fine adjustment of effects upon the workpiece and because it is a safe, simple and effective method for application in production of machine components, machinery and metalwork of various purposes.

The ***Esonix*** technology controls the quality, properties and characteristics of the surface, modifies material properties in the treatment area, improves the fatigue and corrosion resistance, as well as the resistance to abrasion and contact failures, reduces residual stresses and deformations, stabilizes and improves static quality and reliability characteristics in mechanical engineering.

Since plastic deformation is one of effects accompanying this method, interest in UIT has resulted in analogies between UIT and other conventional deformation treatment methods such as shot peening (SP), hammer peening (HP) and ultrasonic shot peening. An experimental comparison of these and other methods made in collaboration with Prof. V.I. Trufyakov and Prof. P.P. Mikheev of Paton Institute (Ukraine) has demonstrated that UIT is the most beneficial method. A summary of the results of this study [16] is shown in Fig. 1.

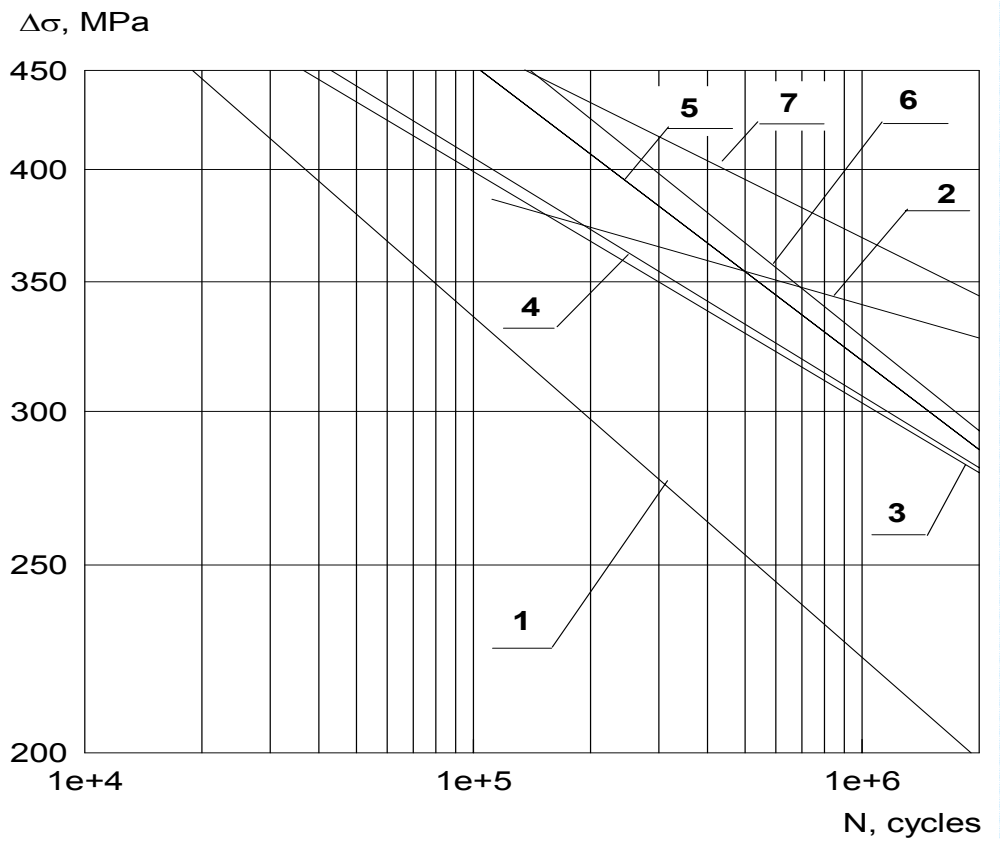

Fig. 1 Fatigue curves for welded joint in steel Weldox 420 in the as-welded and improved conditions: 1 – as welded, 2 – UIT treated using indenters of diameter 3 mm and 5 mm, 3 – hammer peened, 4 – shot peened, 5 – TIG dressed, 6 – TIG dressed and UIT treated using indenters of diameter 5 mm, 7 – UIT treated using indenters of diameter 3 mm.

UIT has radically improved the fatigue limit of welded joints made of different materials under various conditions including aggressive environments and subzero temperatures. These materials include carbon average-strength steels [14, 16, 18-20], high-manganese steels [14], high-strength steels [17, 22], titanium alloys [14], aluminum alloys [18, 22], and bronze [22]

The results of the UIT effect on the fatigue of welded joints in high-strength steel with yield strength of 700 MPa are exemplified in Figs. 2 and 3.

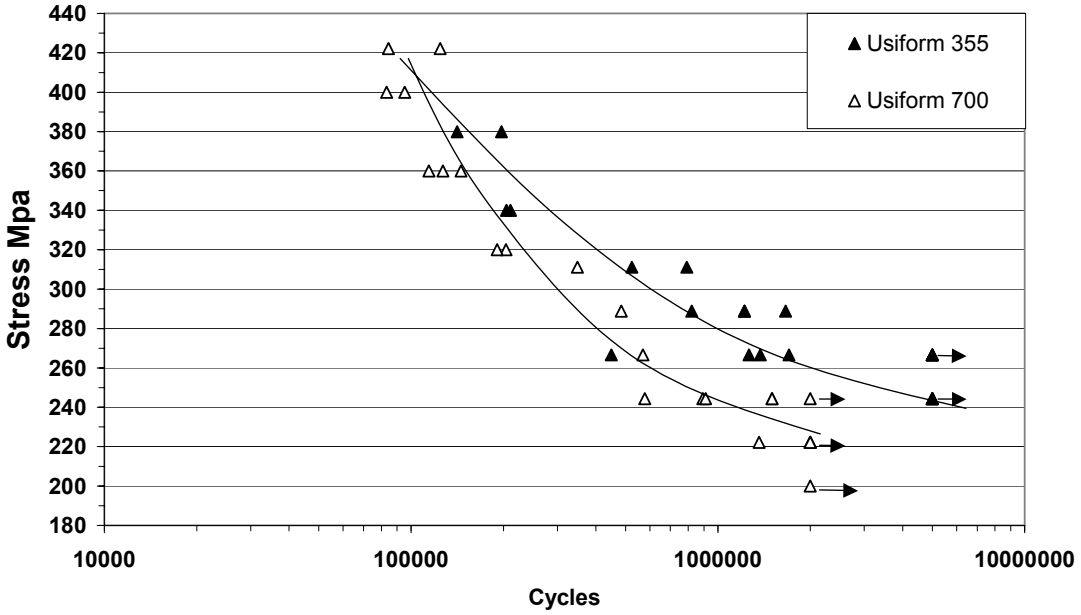

Fig. 2 SN curves for as-welded specimens

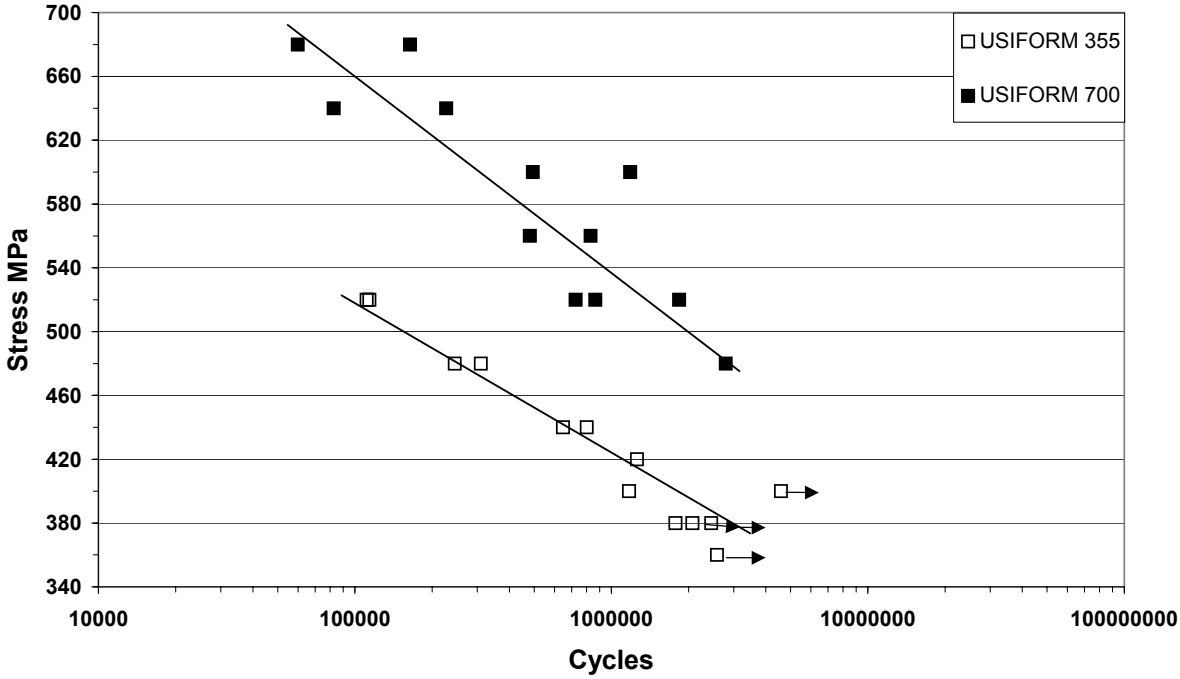

Fig. 3 Comparison of fatigue strengths for UIT joints

The comparative fatigue test results obtained from the as-welded joints in average-strength and high-strength steels are shown in Fig. 2. These results have confirmed that the application of high-strength steels in welded structures under variable loading conditions is not practical.

UIT has changed this by improving the fatigue limit of welded joints in high-strength steel by at least 2 times (Fig. 3) and in fact opened the market of welded structures for high-strength steels.

The results presented above have been approved by Commission XIII. The areas of the UIT effect on the properties and condition of the treated material are described in [14, 15]. Further, the physical features of UIT will be addressed that are directly responsible for the benefits of the method. Note that the UIT benefits are associated with the deformation, relaxation and modification effects upon the material, specifically welded joint material.

3. EXPERIMENTAL AND THEORETICAL STUDY OF UIT DEFORMATION EFFECTIVENESS

This section presents the results of the experimental and theoretical study [23] on the efficiency of the following impacts: random impacts caused by a single impulse of force as defined in [24] with boundary conditions of hammer peening, the impact with boundary conditions of ultrasonic hammer peening as defined in [25] and ultrasonic impact as defined in [4]. A dynamic model of the ultrasonic impact as defined in [4] and the impact as defined in [25] is also addressed.

Let us first define that the ultrasonic impact upon the impact object in accordance with [4] and [15] occurs under the action of the impulse of force (generated by ultrasonic transducer vibrations) at the rear end of a freely axially moving needle indenter with a normalized wave length directly contacting the transducer tip and the impact surface. At this impact phase, the indenter vibrates ultrasonically with a rebound from the surface, as well as synchronously and in-phase with ultrasonic transducer vibrations at its resonance frequency that is responsible for the carrier frequency in the impact spectrum and causes impact surface to vibrate adequately to the carrier frequency in the impact area without indenter rebounding from the initiating transducer tip and the impact surface being initiated.

Thus, the ultrasonic impact, along with plastic deformation of the surface material and stress impulse generation in the subsurface material, is accompanied by ultrasonic plastic deformation of the surface material and ultrasonic stress wave generation in the subsurface material.

At the same time, the impact caused by a single impulse of force creates the area of plastic deformations on the impact surface and provides for stress impulse propagation in the subsurface material.

The method we proposed to compare the impact efficiency is based on the comparison of the results of surface plastic deformation with single impact conditions being the same. This also includes the comparison of the indenter mass and geometry, which are responsible for the contact resistance of the surface material to equivalent dynamic loading.

The effect of the geometry of the needle indenter (as defined in [4]) and ball indenter (as defined in [25]) on the nature and efficiency of the impact was also evaluated based on the length of the impact responsible for surface plastic deformation.

In all cases the comparison was made between the effects of a single impact realized by means of the device shown in Fig. 4 and a synchronous termination of excitation at the output of the ultrasonic generator at the instant when the indenter starts rebounding from the surface.

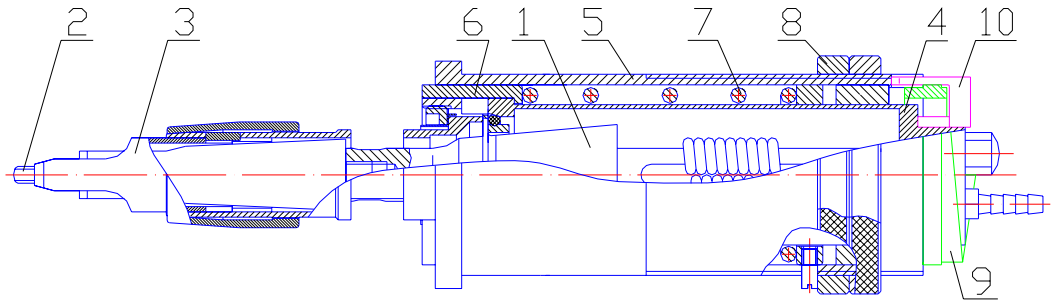

Fig. 4 Device for realization of a single impact

The device shown above operates as follows. The spring 7 is preliminary loaded to install the ultrasonic transducer 1 (located in the cooling jacket 4) with a rigidly attached concentrator 3 and a freely axially moving indenter 2 positioned at a specified distance from the impact surface. The spring is loaded by turning the end tappet 9 relative to the casing 5 and a simultaneous movement of a shaped key 10 fixed in the jacket 4.

Upon the spring release, the mass movable relative to the casing creates the impact impulse that remains constant in all experimental variations specified.

The spring is precompressed by means of the adjusting nut 8 before loading. The shaped key protects the turning of the movable mass in the casing during loading and releasing the spring. The friction conditions for components moving in the casing are the same. This is due to a negative reverse angle of 5° at the trailing edge of the end tappet.

The friction conditions for various indenters were identical because indenter holders were made of the same material (tool steel) with a specified accuracy and surface roughness of the guide channel.

The experimental conditions of acoustic energy transfer from the transducer to the impact surface were the same, while different types of indenters were used. Specifically, the concentrator tip for a ball indenter had a spherical indentation of such a depth and radius that the area of this indentation was equal to that of the rear end of the needle indenter. The radius of the working end of the needle indenter, in turn, was equal to the radius of the ball indenter. Masses of both indenters were also equal. All indenters were made of the same material and their working surface had the same hardness and roughness.

Table 1 Indenter dimensions

No.	Type	Radius of work surface, mm	Length, mm
1.	Needle ∅6.35 mm	4	25
2.		4	9.2
3.		5	17.1
4.		6	29.0
5.	Ball	4	-
6.		5	-
7.		6	-

The impact efficiency using indenters given in Table 1 was evaluated under the following initial conditions:

- a preset pressing force of the tool movable mass against the impact surface – 0, 5, 10, 15 and 25 kg;
- before impacting the tool movable mass is withdrawn from the surface by 2 and 10 mm;
- a vibrational amplitude of the waveguide tip under no-load conditions – 0 and 50 μm.

Indenters given in table by No. 1 were used to compare the efficiency of the ultrasonic impact and the impact caused by a single impulse of force. Nos. 2-7 are indenters having equal masses and work surface radiuses.

Specimens were made of aluminum alloy AlMg5 and steel 20.

The statistical reproducibility of the results was evaluated prior to testing (7 measurements for each variation of impact). The scatter of the results obtained from measuring and calculation of the indentation area and volume did not exceed one percent.

The following was controlled during testing:

- the indentation diameter;
- the length of the double-side impact;
- the length of the single impact upon the impact surface.

The indentation diameter was evaluated using measuring microscope to the three-place accuracy.

The area of indentation was calculated by:

$$S = 2\pi Rh$$

where:

R is the radius of the indenter working surface;

a is the indentation diameter;

$h = R - \sqrt{R^2 - \frac{a^2}{4}}$ is the indentation depth.

The indentation volume was calculated by:

A sample estimate was made for indentation volume using the weight method. For this purpose, indentations were filled with plasticine and the moulds were weighed thereafter. The results obtained have confirmed the calculation data.

The length of impact was controlled using an oscilloscope connected to the contact sensor.

The results are presented in diagrams, showing the relationship between the impact efficiency in terms of the area and volume of indentations made by different indenters and initial impact conditions mentioned above.

It can be seen that indentation dimensions are virtually independent of the type of indenter under ultrasonic-free impact conditions using indenters with the same work surface radius (Figs. 4 and 6).

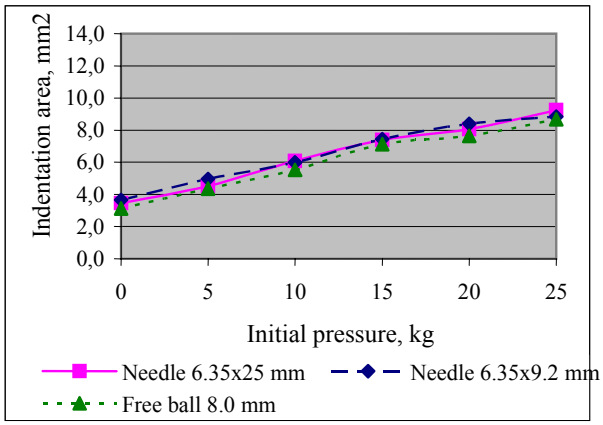

Fig. 5 Indentation area on ultrasonic-free impacting upon aluminum alloy specimen using indenters with working surface radius of 4 mm when the movable mass is withdrawn from the surface by 10 mm

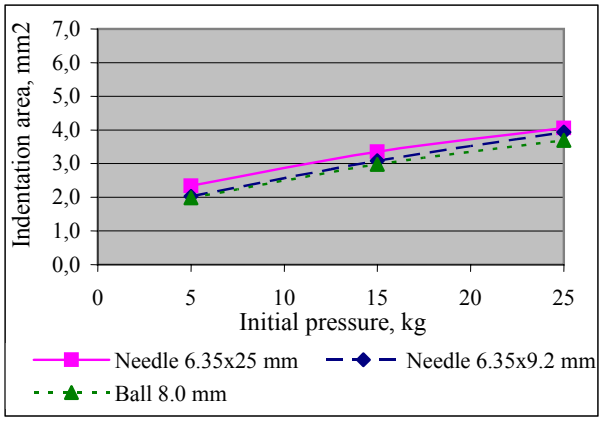

Fig. 6 Indentation area on ultrasonic-free impacting upon steel specimen using indenters with working surface radius of 4 mm when the movable mass is withdrawn from the surface by 10 mm

At the same time the ultrasonic vibrations of the indenter create plastic deformation at the instant of impact. This is confirmed by a respective increase of the area and volume of indentation. Fig. 7 shows that when the concentrator tip is withdrawn from the rear end of the indenter at a distance close to the actual impact amplitude during UIT or HP, being equal to 2 μm, the ultrasonic impact, as compared to the single impact appropriate to hammer peening, increases the indentation area by up to seven times over the entire range of the initial experimental conditions.

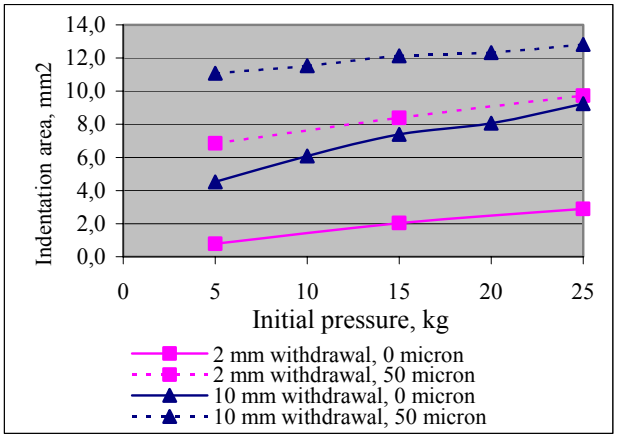

Fig. 7 Indentation area on ultrasonic and ultrasonic-free impacting upon aluminum specimen using needle indenter ∅6.35x25 mm with working surface radius of 4 mm when the movable mass is withdrawn from the surface by 2 and 10 mm

The analysis of the impact efficiency by different indenters in terms of the magnitude and distribution of microhardness has shown that the ultrasonic impact by the needle indenter increased the microhardness of the aluminum specimens from HV_{20} 64 to HV_{20} 80, while impacting by the ball indenter up to HV_{20} 72. In the former case the depth of hardening is 0.4 mm, and in the latter case 0.3 mm. It should be considered that the results were obtained by a single impact and that these determine the treatment effectiveness and performance in depth in the non-linear proportion to the impact length and treatment time. We have already demonstrated [16-18, 21, 21] that UIT hardens the materials of this sort to the depth of up to 2 mm and more.

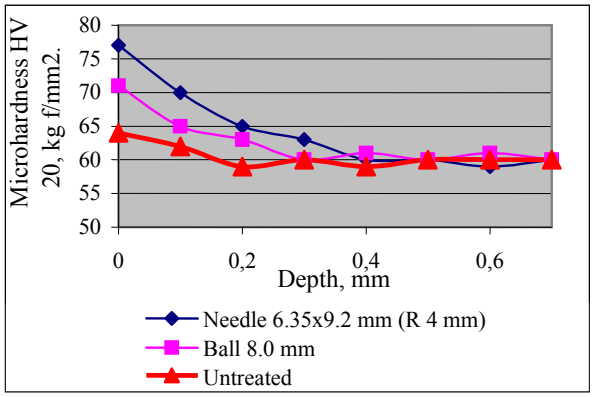

Fig. 8 Microhardness distribution across the thickness of aluminum specimen on impacting using indenter with working surface radius of 4 mm when the movable mass is withdrawn from the surface by 2 mm (vibrational amplitude 50 μm).

Due to size restrictions we cannot present the results obtained for all indenters and all initial experimental conditions of the impact. Thus, we will restrict ourselves to presenting indentation area relationships after impacting steel specimen using indenters with a working surface radius of 5 mm and a withdrawal of 10 mm, referring to that the other results are similar to those presented in Fig. 9.

As can be seen, the efficiency of a single ultrasonic impact by the needle indenter is by 20 to 40% greater than that of the ball indenter. Since this difference will grow with each subsequent impact, the actual impact efficiency will be determined by the impact length.

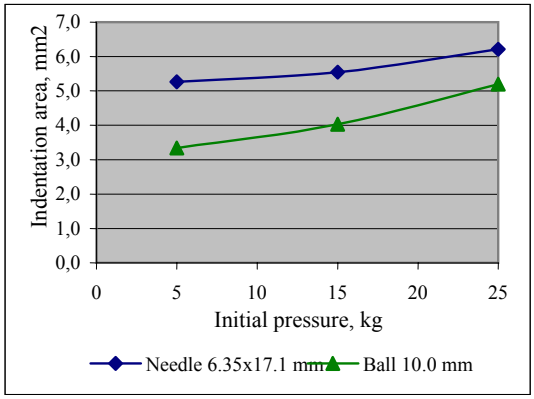

Fig. 9 Indentation area on impacting steel specimen using indenter with working surface radius of 5 mm when the movable mass is withdrawn from the surface by 10 mm (vibrational amplitude 50 μm)

Of particular interest in this study is the comparison of time characteristics of impacts transformed at the impact surface via needle and ball indenters. In addition to the above-mentioned initial conditions, we took into account the chatter suppression. This is not of great importance when impacting upon the needle indenter that has high displacement stability in the guide hole. At the same time, the ball indenter has unlimited freedom of displacement in any direction. These displacements create favorable conditions for chatter with a small (relative to the minimum level of work of plastic deformation) displacement energy. In this experiment a withdrawal of 2 mm and pressure of 50 kg were taken.

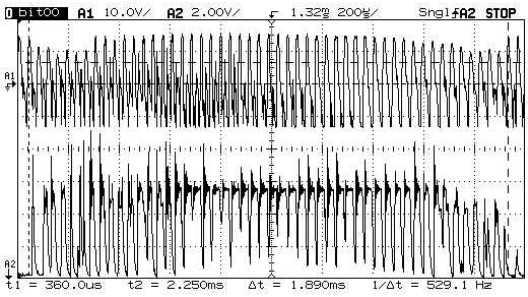

Fig. 10 Oscilloscope picture of transducer excitation (top) and ultrasonic impact excitation (bottom) using needle indenter with working surface radius of 5 mm, pressure of 50 kg and movable mass withdrawal of 2 mm

From oscilloscope pictures shown in Fig. 10 is seen that the needle indenter impact is accompanied by the distinct ultrasonic vibrations in the material of the impact surface. At the same time, from the oscilloscope picture shown in Fig. 11 it can be seen that an excess freedom of motion of the ball indenter causes single rebounds from the impact surface even with higher pressure.

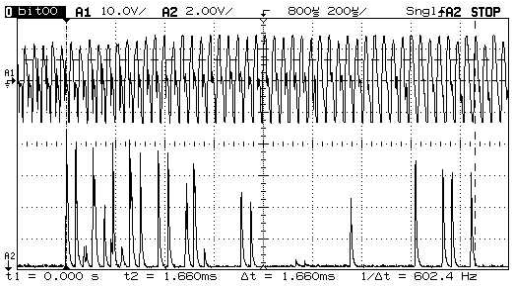

Fig. 11 Oscilloscope picture of transducer and impact excitation using ball indenter with working surface radius of 5 mm, pressure 50 kg and movable mass withdrawal of 2 mm

It should also be taken into account that when the ball is impacted the compressive stresses result in the distribution of a recovery elastic force through the entire area of diametral section that is generally much greater than the indentation diameter. Moreover, the needle indenter produces the indentation with diameter much closer to that of the indenter as compared to the ball of equal mass. Thus, additional elasticity occurs in the ball indenter (relative to the needle indenter), which causes the ball indenter to rebound earlier.

This confirms that the authors of [25] calling their methods as ultrasonic hammer peening are right. This method really differs from the UIT method by its physical features defined by the system of single impact impulses with a relatively low repetition rate and the length less or close to that of one period of ultrasonic vibrations. At the same time, the length of ultrasonic impact is determined by tens of periods of indenter ultrasonic vibrations, synchronous and in-phase vibrations of the impact surface material in the area of ultrasonic impact.

3.1 Dynamic model of impact

At any instant of time the stressed state is calculated using the global stiffness matrix $\sum_{i=1}^{k}\left[K^{(e)}\right]$,

where K = the number of finite elements in the model; *(e)* = the total number of degrees of freedom of points of the finite elements. The variation of the model state with time is described by direct calculation of discrete values of stress-strain function in the oscillating system with lumped parameters (OSLP), as well as by taking into account the effect of an external harmonic force on the elements of the oscillating system with distributed parameters (OSDP) coupled by this force. It is agreed that the initial experimental conditions described above are valid for both oscillating systems. It was found that OSLP corresponds to the movable mass with a spring and OSDP to the indenter rigidly attached to the impact object by an external harmonic force.

The model design [23] is accomplished, provided that each finite element is in equilibrium. The summary stiffness matrix of the finite element is as follows:

$$\left[K^{(e)}\right] = \int [\beta]^T [E][\beta] dV ,$$

where:

dV = increment (or decrease) of the finite element volume;
$[\beta]$ = deformation matrix of a finite element;
$[K^{(e)}]$ = stiffness matrix of a finite element;
$\xi\eta\zeta$ = space of non-dimensional coordinates;
$\underset{\rho}{U}^{(e)}$ = resultant vector of free displacements of finite element points;
$\underset{\rho}{u}(\underset{\rho}{r})$ = displacement field of all finite element points;
Ψ_r = finite element geometry function;
$\underset{\rho}{\varepsilon}(\underset{\rho}{r})$ = strain field between all points of a finite element;
$\underset{\rho}{\sigma}(\underset{\rho}{r})$ = stress field between all points of a finite element;
$[E]$ = matrix notation of the coefficient of elasticity, allowing for all types of deformation (compression, tension, shearing, torsion).

Assuming that Fig. 10 shows the sought-for finite element consisting of 8 points and that it may be transformed into 4, 5, 6, and 7-point element by combining the points, the construction of deformation matrix $[\beta]$ of any 8-point finite element may be accomplished in the following order

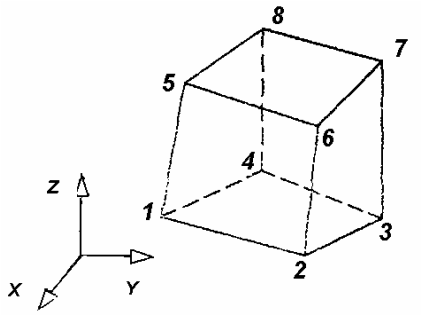

Fig. 12 Sought-for finite element

Any T-D element in the space of non-dimensional coordinates $\xi\eta\zeta$ with facets in six planes ($\xi=\pm1$, $\eta=\pm1$, $\zeta=\pm1$) may be described by the set of equations in space XYZ:

$$\begin{cases} x(\xi,\eta,\varsigma) = \sum\limits_{r=1}^{8} \Psi_r(\xi,\eta,\varsigma) x_r \\ y(\xi,\eta,\varsigma) = \sum\limits_{r=1}^{8} \Psi_r(\xi,\eta,\varsigma) y_r \\ z(\xi,\eta,\varsigma) = \sum\limits_{r=1}^{8} \Psi_r(\xi,\eta,\varsigma) z_r \end{cases},$$

where $\Psi_r(\xi,\eta,\zeta) = \frac{1}{8}(1+\xi_r\xi)(1+\eta_r\eta)(1+\zeta_r\zeta)$ is the form function.

The displacement field $\underset{\rho}{u}(\underset{\rho}{r})$ written by the form function is as follows:

$$\underset{\rho}{u}(\xi,\eta,\varsigma) = \sum_{r=1}^{8} \Psi_r(\xi,\eta,\varsigma) \underset{\rho}{v}_r .$$

The deformation field $\underset{\rho}{\varepsilon}(\underset{\rho}{r})$ is:

$$\underset{\rho}{\varepsilon}(\xi,\eta,\varsigma) = \sum_{r=1}^{8} [\beta] \underset{\rho}{v}_r = [\beta] \underset{\rho}{U}^{(e)}$$

Then,

$$[\beta_r] = \begin{bmatrix} \frac{\partial \Psi_r}{\partial x} & 0 & 0 \\ 0 & \frac{\partial \Psi_r}{\partial y} & 0 \\ 0 & 0 & \frac{\partial \Psi_r}{\partial z} \\ \frac{\partial \Psi_r}{\partial y} & \frac{\partial \Psi_r}{\partial x} & 0 \\ \frac{\partial \Psi_r}{\partial z} & 0 & \frac{\partial \Psi_r}{\partial x} \\ 0 & \frac{\partial \Psi_r}{\partial z} & \frac{\partial \Psi_r}{\partial y} \end{bmatrix};$$

and $[\beta] = [[\beta_1] \text{K} [\beta_8]]$ is the sough-for deformation matrix of the 8-point element.

The elastic matrix may be further constructed, provided that finite element deformations are small.

Since the Hooke's law is true for relatively small deformations, the following is true between $\vec{\varepsilon}$ and $\vec{\sigma}$ (E = coefficient of elasticity, G = shear modulus, μ = Poisson's ratio):

$$\sigma_x = \frac{E}{(1+\mu)(1-2\mu)}((1-\mu)(\varepsilon_x + \mu(\varepsilon_y + \varepsilon_z));$$

$$\sigma_y = \frac{E}{(1+\mu)(1-2\mu)}((1-\mu)(\varepsilon_y + \mu(\varepsilon_x + \varepsilon_z));$$

$$\sigma_z = \frac{E}{(1+\mu)(1-2\mu)}((1-\mu)(\varepsilon_z + \mu(\varepsilon_x + \varepsilon_y));$$

$$\tau_{xy} = G\gamma_{xy};\ \tau_{xz} = G\gamma_{xz};\ \tau_{yz} = G\gamma_{yz};$$

In matrix form, these equations are of the form $\vec{\sigma} = [E]\vec{\varepsilon}$, where

$$[E] = \frac{1}{(1+\mu)(1-2\mu)} \begin{bmatrix} 1-\mu & \mu & \mu & 0 & 0 & 0 \\ \mu & 1-\mu & \mu & 0 & 0 & 0 \\ \mu & \mu & 1-\mu & 0 & 0 & 0 \\ 0 & 0 & 0 & \frac{1-2\mu}{2} & 0 & 0 \\ 0 & 0 & 0 & 0 & \frac{1-2\mu}{2} & 0 \\ 0 & 0 & 0 & 0 & 0 & \frac{1-2\mu}{2} \end{bmatrix};$$

Thus, all functional arguments of the global stiffness matrix are found. The model makes it possible to analyze and show the change of the stress field in the indenter and impact object during impact under the effect of external forces and initial conditions specified above. Discrete modes of deformation for pairs "indenter-impact object" are shown in Fig. 11.

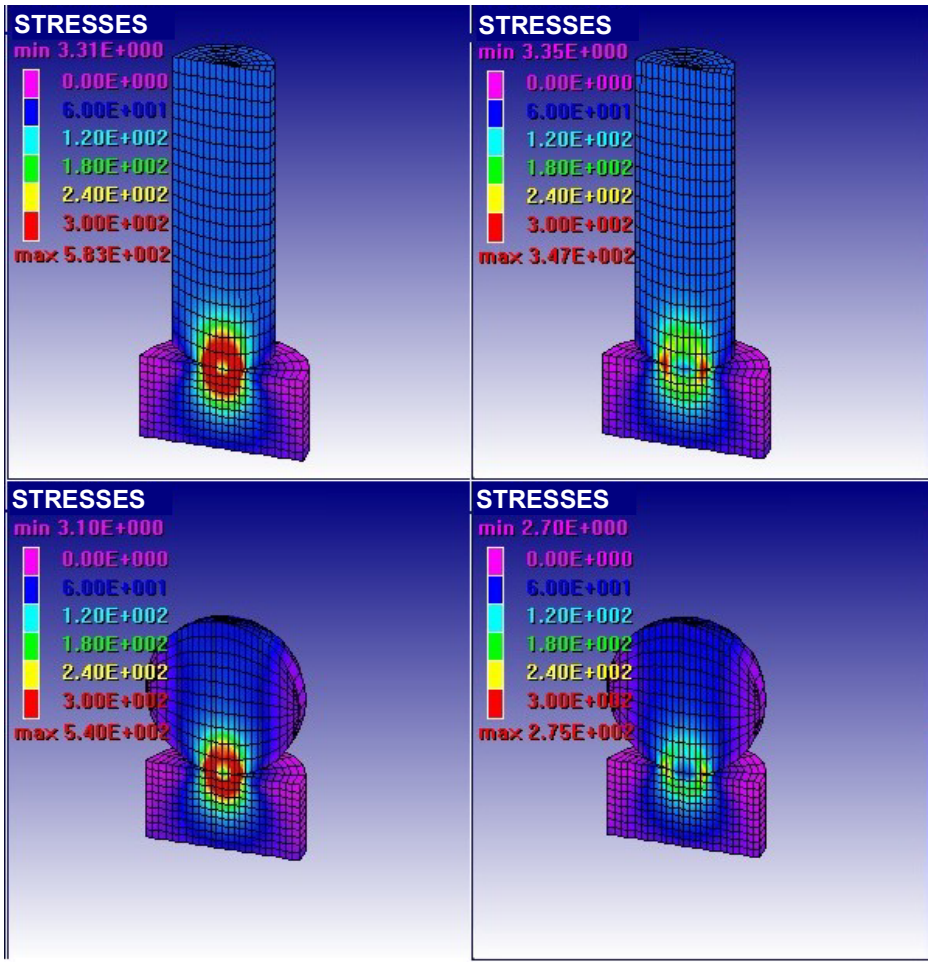

a) "Parallel operation" of indenters

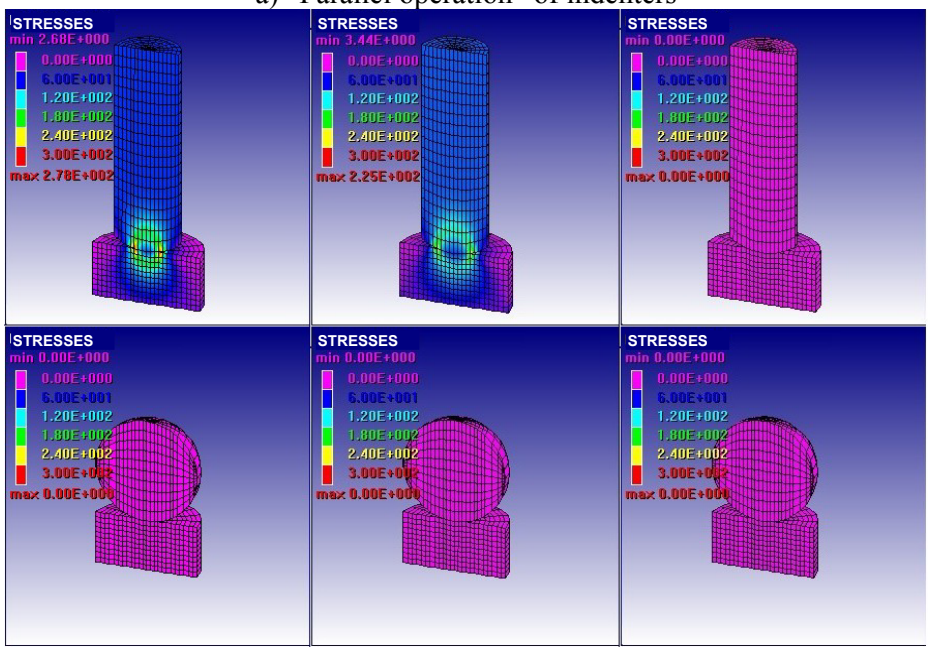

b) Early rebound of the ball indenter and continuing "operation" of the needle indenter

Fig. 13 Discrete representation of ultrasonic impact by the needle indenter and impact by the ball indenter

The analysis of the impact efficiency based on the impact length was made using a dynamic model. The analysis result is shown in Fig. 14. By comparing the dynamics of embedding indenters into the material being impacted it can be seen that the ball indenter displacement ceases as the impact force, expressed using contact stresses, decreases, while embedding of the needle indenter continues. The flatter portion of the curve shows the effect of ultrasonic plastic deformation.

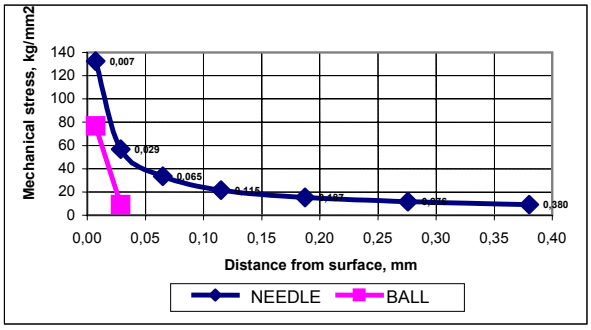

Fig. 14 Comparison of efficiency between ultrasonic impact by the needle indenter and single impacts by the ball indenter

Thus, it is shown that the greater efficiency achieved due to impact by the needle indenter is as a result of the following advantages it has over the ball indenter: localization of the impact energy, impact length, and the ultrasonic phase synchronous to the sought-for impact.

3.2 Basic Conclusions

1. Along with impulse deformation of the impacted surface, the ultrasonic impact is accompanied by ultrasonic deformation of the surface, modification of material properties and the generation of ultrasonic wave within the workpiece material.

2. These properties of the ultrasonic impact define its greater efficiency as compared to other methods of surface deformation.

3. The ultrasonic impact by the needle indenter fundamentally changes the nature of the interface and interaction in the oscillating system: ultrasonic transducer – indenter – impact object. The main distinctive feature of such an interaction is defined by the time phases of the ultrasonic impact: a) ultrasonic vibrations of an indenter in a gap between the transducer tip and the surface being treated, b) in-phase continuous (without detachment) ultrasonic vibrations of an indenter in synchronism with these surfaces. The duration of the ultrasonic impact is greater than that of the single impact by an order of magnitude and more.

4. EXPERIMENTAL STUDY OF THE UIT MECHANISM

It is shown above that the ultrasonic impact is accompanied by greater deformation effect upon the surface in comparison with a single impact. This experimental observation is supported by the impact dynamic model [16], which in turn interprets two parallel effects that accompany the ultrasonic impact: reduction of deformation resistance and extension of time of the impact action upon the surface due to ultrasonic vibrations of the indenter with and without rebounding from the initiating output surface of the transducer and the impact surface. That is, the UIT effectiveness is directly related to the ultrasonic vibrations of the indenter during action upon the surface.

It should be noted that the effects of the deformation resistance reduction under ultrasonic action were established by F. Blaha and B. Langenecker in 1950s [26], E.G. Konovalov in 1960s [27], L.D. Rosenberg, V.F. Kazantsev [28] and other researchers of that period. Their works demonstrated that ultrasonic vibrations activate relaxation of modes of deformation caused by processing factors and external forces upon different materials. However, the level of the development of ultrasonic oscillating systems and methods of ultrasound introduction, which required high quality surface finish for treated solid bodies to ensure a reliable acoustic contact between the transducer and the object, did not allow a wide application of the then achievements industrially. In spite of this, as early as in 1970s the optimization of the magnetostrictive transducers [1, 29, 30] created conditions for application of high-intensity ultrasound, specifically which is initiated by the ultrasonic impact, in manufacture of welded structures and specific-purpose machinery components. These applications were preceded by investigations that confirmed the effective transfer of ultrasound into the treatment object through the area of plastic deformations [31], as well as the reduction of the deformation resistance and relaxation activation under ultrasonic action caused by the ultrasonic impact [32]. Let us next present the basic results of these investigations.

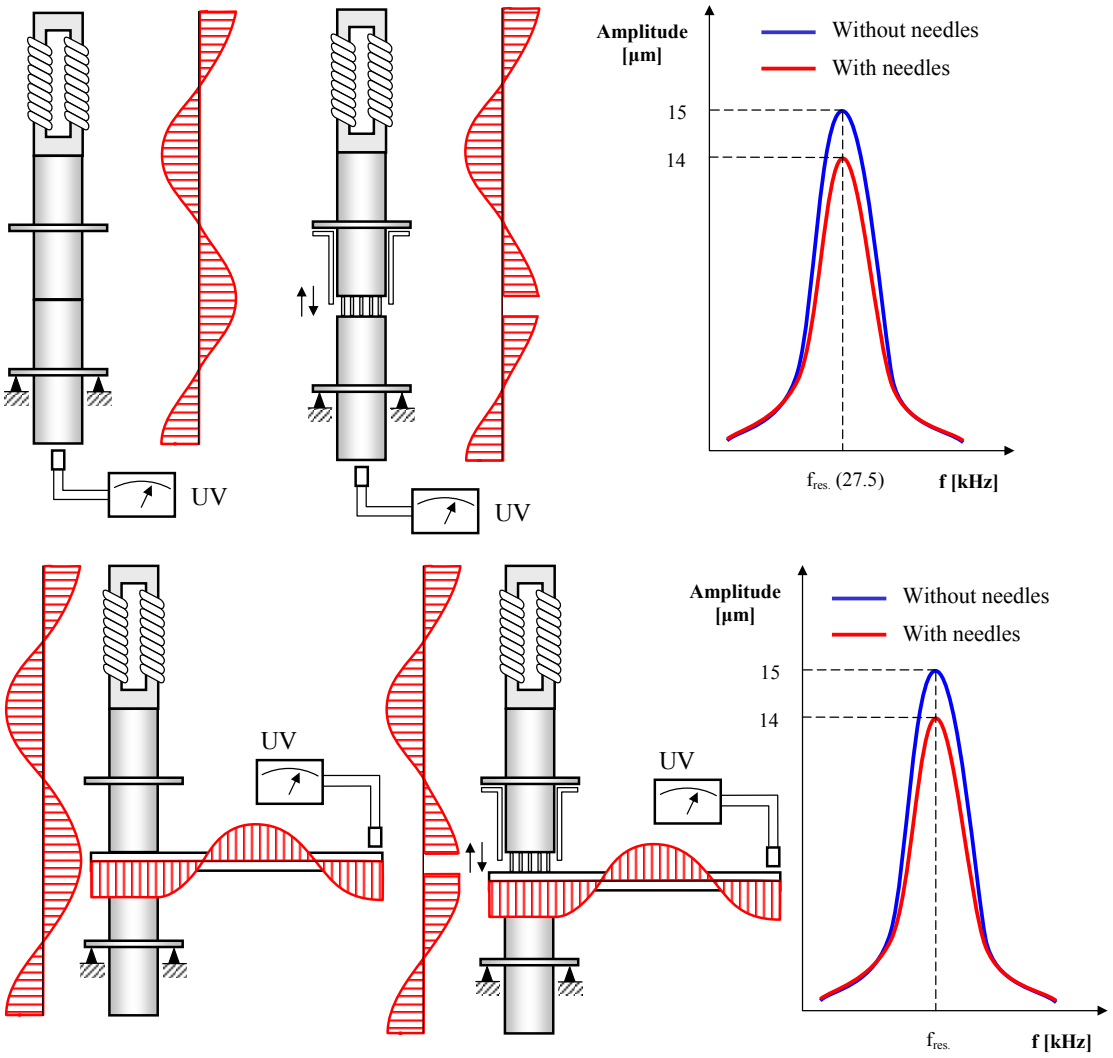

Fig. 15 Efficiency of oscillation excitation by ultrasonic impact tool in resonance models

One can see a highly beneficial ultrasonic oscillation energy transfer in a resonance system by means of the ultrasonic impact [1] via a freely axially moving indenter through the plastic deformation region with low coupling between the transducer and the waveguide. The results obtained are equally verified for conditions of longitudinal and flexural wave transfer.

The main merit of the method of transferring ultrasound into objects via ultrasonic impact is its low sensitivity to the initial state of the surface during impulse introduction of high-intensity ultrasonic vibrations.

These results allowed us to progress directly to the study of the effect of the ultrasonic impact on the deformation resistance reduction in comparison with a direct acoustic contact of the transducer and the object, see Fig. 16.

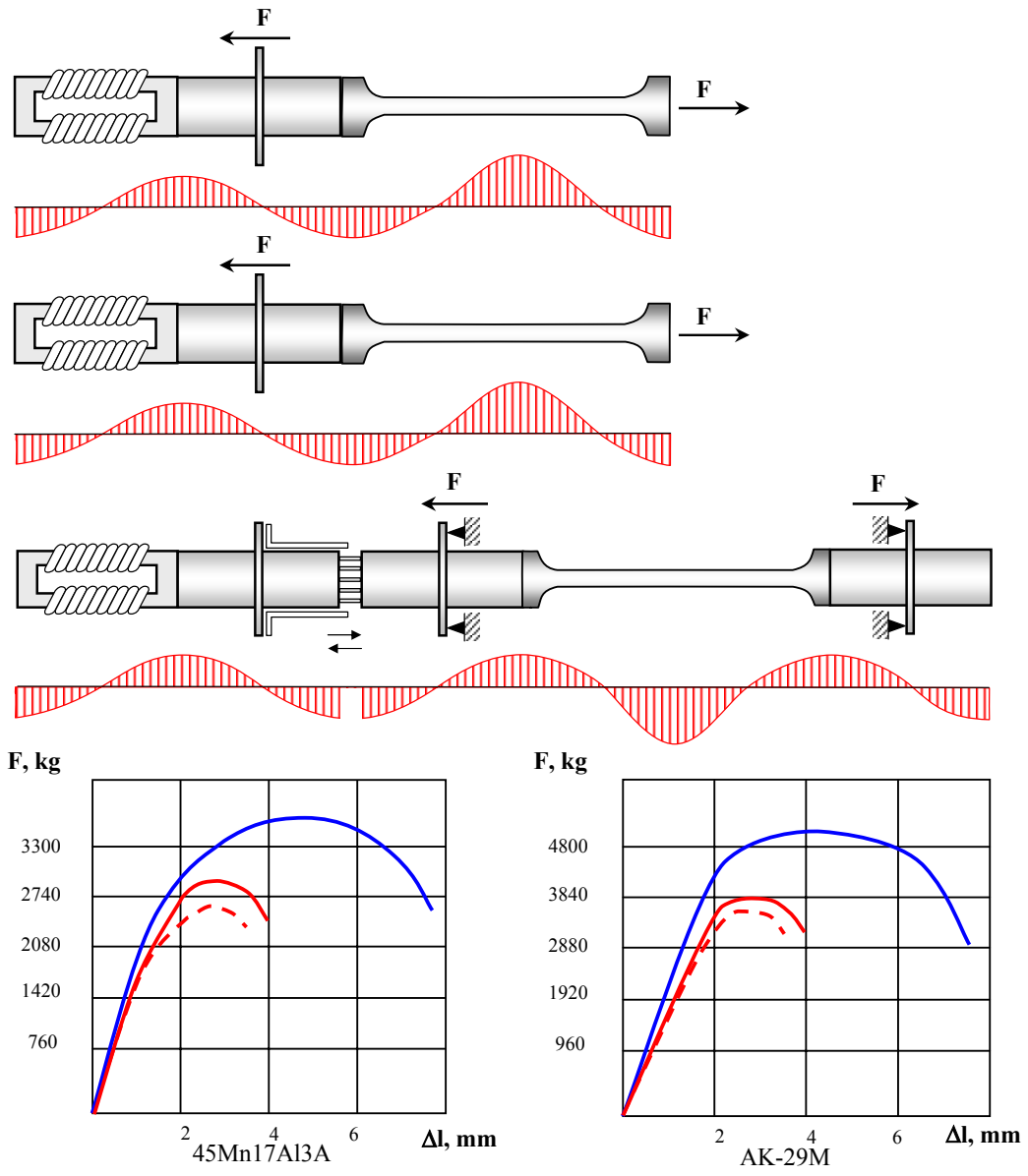

Non-infonified samples
Insonified samples with a direct contact with a concentrator
Samples insonified via free indenters (ultrasonic impact).

Fig. 16 Tension activation by means of ultrasound with different modes (and levels) of acoustic coupling

Experimental conditions:
1. Materials: Manganese steel 45Mn17Al3A with yield strength of 45 kg/mm^2 and heat-strengthened steel of perlite class AK-29M with yield strength of 65 kg/mm^2.
2. The deformation extent was specified and the deformation resistance measured.
3. Tension under simultaneous excitation of ultrasonic vibrations in a resonance sample. Frequency F = 44 кГц, Vibrational amplitude A = 18 μm, sample diameter = 10 mm.

As is seen, with a general reduction in tensile strength under ultrasonic action by 27-30%, this reduction is 24-26% in the case of the ultrasonic impact. Note that in this experiment the fixing conditions of the resonant system being impacted have restricted the possible increase in amplitude of ultrasonic vibrations that allow a greater reduction in deformation resistance. Nevertheless, the results obtained have confirmed the effective introduction of ultrasound into the resonance sample by means of the ultrasonic impact to reduce tensile resistance.

The creep is an important factor of stress relaxation in materials. Fig. 17 shows the results of the creep evaluation for manganese steel under the action of temperature and ultrasonic vibrations initiated through a direct communication with a transducer and ultrasonic impact.

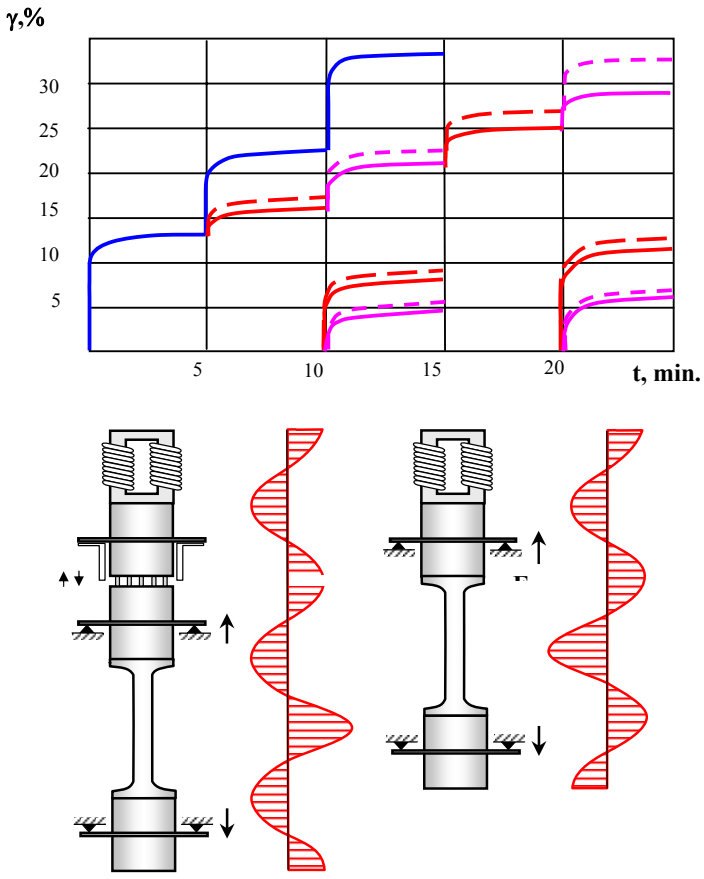

Creep under static loading only

Ultrasonically enhanced creep with a direct contact with concentrator, F=27 kHz, A=10 μm

Creep enhanced by ultrasound via freely moving indenters, F= 27 kHz, A=10 μm

Creep of sample insonified under direct contact with a concentrator and caused by increase in static load by σ=1 kg/mm2

Creep of sample insonified via freely moving indenters and caused by increase in static load by σ=1 kg/mm2

Sample is made of steel 45Mn17Al3 (yield strength at 20°C is 39-42 kg/mm2, tensile strength is 59-62 kg/mm2).
7 sets comprising 7 samples each at a constant test temperature in accordance with the creep time. The figure shows the statistical data.
Sample diameter is 10 mm.
Test temperature is 300°C.
At the test temperature, initial tensile forces are 0.7, 0.5-0.6 and 0.3-0.4 of yield strength (29-31 kg/mm2).
A stage increase in force is 5% of the previous level.

Fig. 17 Creep activation by ultrasound with different modes (and levels) of acoustic coupling

As can be seen, once the sample is in a stable state, which is expressed through its elongation under static force (constant mass), ultrasonic vibrations, with a direct acoustic contact, activate the creep to 30% relative to the elongation obtained earlier. Under normal conditions, the ultrasonic impact provides at least 25% elongation of the same level of static elongation of a sample.

The creep initiated by ultrasonic vibrations under ultrasonic impact and direct acoustic contact conditions is shown in Fig. 18.

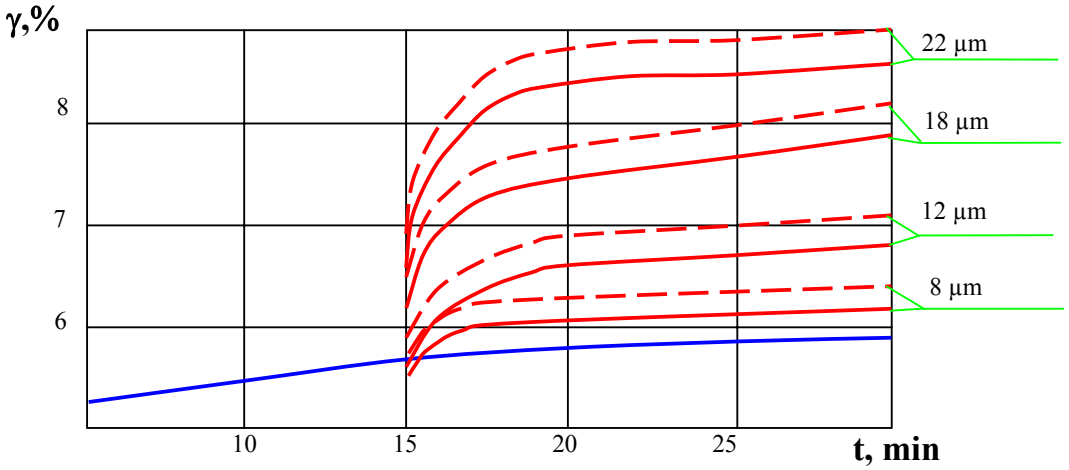

Fig. 18 Creep activation by means of ultrasound with different modes (and levels) of acoustic coupling

As seen above, the ultrasonically initiated creep activation effects under ultrasonic impact and direct acoustic contact conditions differ by no greater than 15%.

Thus, it is shown that the ultrasonic impact is accompanied by high-power ultrasonic vibrations and ultrasonic stress waves that suffice to modify material condition as specified by the task.

These results allowed us to progress to the evaluation of the achievable level of relaxation of the welded joint mode of deformation.

The idea of the experiment shown in Fig. 19 was to compare the effect of ultrasound, initiated by the ultrasonic impact, upon the tensile strength in a reference sample with the residual stress relaxation in a sample under study, which was rigidly fixed during welding. The ease of the ultrasound introduction by means of the ultrasonic impact enabled welding operations and stress measurement preparation in a jig that was subsequently installed, together with a sample, on a stand for ultrasonic impact treatment, as shown in Fig. 19. The sample was made of titanium alloy 48OT3, which was chosen from processing and acoustic-mechanical considerations: high-quality welding using a non-consumable electrode with a filler and argon as a shielding gas, the weld face having minimum irregularities; high Q-factor = 5000; employing tested and optimized stress measurement procedures. The sample had a diameter of 20 mm and the resonant length of 115 mm, depending on the sound speed in a specific range of products.

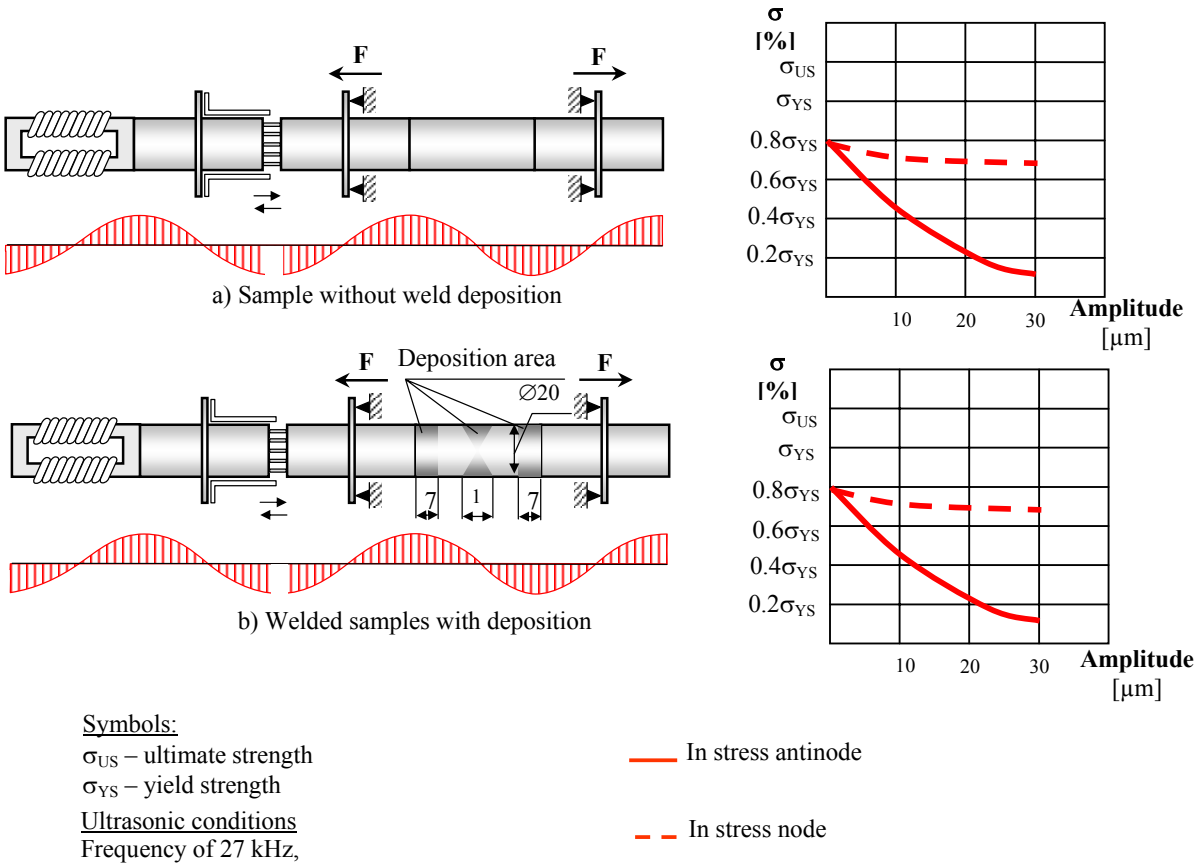

Fig. 19 Ultrasonically assisted stress reduction in a system with low acoustic coupling

Experimental conditions:

1. The sample shown in Fig. 19b was welded so that no welding distortion was allowed (rigid fixation).
2. Following UIT treatment, residual welding stresses were measured by X-ray diffraction method. Depending on the ultrasonic vibrational amplitude, residual stresses were measured on a rigidly fixed resonance sample in antinode and node areas of ultrasonic displacements (or stresses). The portable X-ray apparatus URS-55 having a fine focus tube was used for stress measurements.
3. In-process stress measurements during welding and UIT were made using strain gages on a sample fixed in a jig. The gages were installed on load-carrying ribs of a rigid jig used for welding and UIT treatment.

Thus, it is shown that the level of residual welding stress relaxation by ultrasonic impact treatment is consistent with the level of residual stress reduction during heat treatment and attains 10-15% of the yield strength of the material being treated.

A similar procedure was used to evaluate the ultrasonic impact effect on the modification of the non-resonant sample condition. Such data, including relaxation and replacing tensile stresses by compressive stresses, were obtained from rigid non-resonant in thickness plates made of carbon steels of various strength, titanium alloys, aluminum alloys, and copper. The data obtained are shown in Fig. 20 taken from [7] to facilitate the comparison of the results. As seen from Fig. 20, the change of impulse and damped ultrasonic stresses acting deep in the material and initiated by

the ultrasonic impact is of an exponential nature relative to the maximum compressive stresses and ultrasonic contact stresses at a sample surface in the area of plastic deformations caused by UIT.

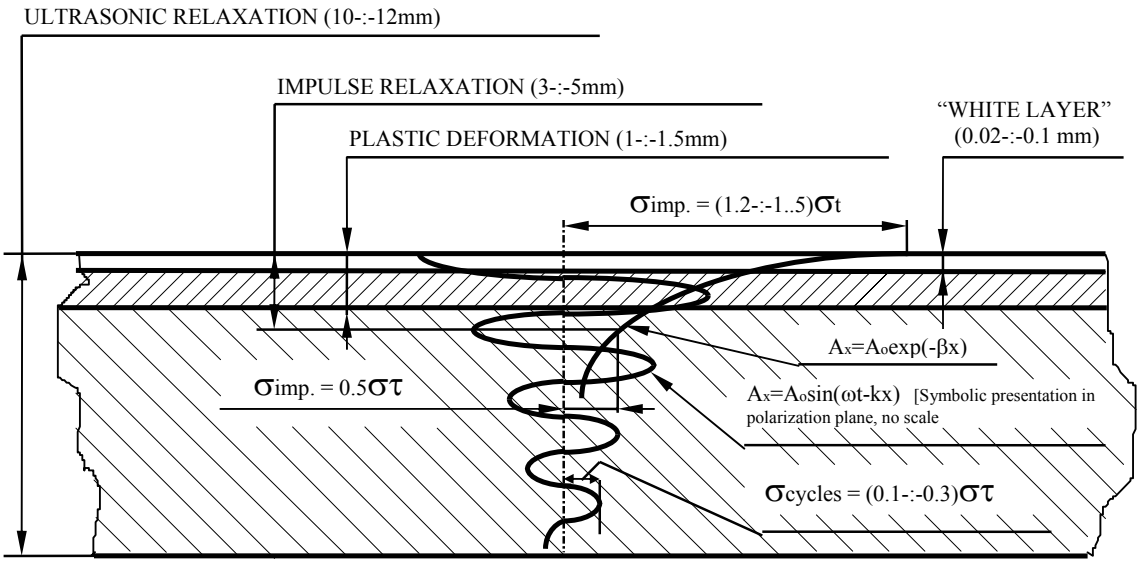

ZONES	TECHNICAL EFFECT
"White layer"	Wear-resistance, corrosion resistance
Plastic deformation	Cyclic endurance, compensation of deformation, corrosion-fatigue strength
Impulse relaxation	Reduction in residual welding stress and strain of up to 70% of the initial state
Ultrasonic relaxation	Reduction in residual welding stress and strain of up to 50% of the initial state

Fig. 20 Physical zones of UIT effect on material properties and condition

In this section, we will restrict ourselves to a general representation of the technical effects (see Table above) caused by ultrasonic plastic deformation, impact impulses and ultrasonic stress waves associated with the ultrasonic impact in the material, since these directly stem from the experimental results presented above. Because the "white layer" formation mechanism [14] is associated to a greater extent with the contact conditions in the ultrasonic impact area, which are described by special methods, we will restrict our discussion to the finite data obtained on 10Mn2VBe steel and shown in Fig. 21.

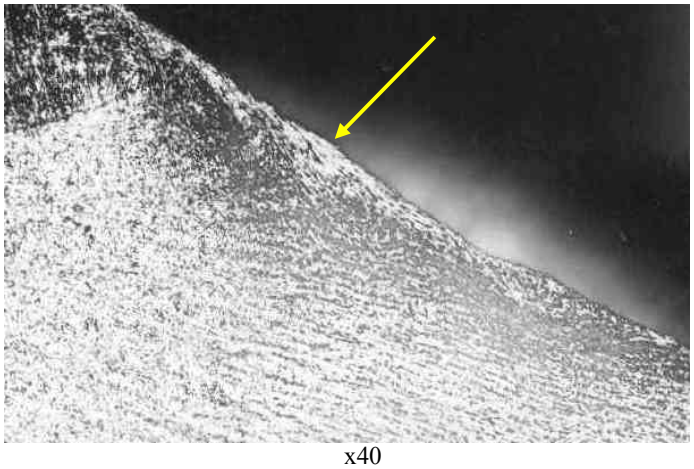

x40

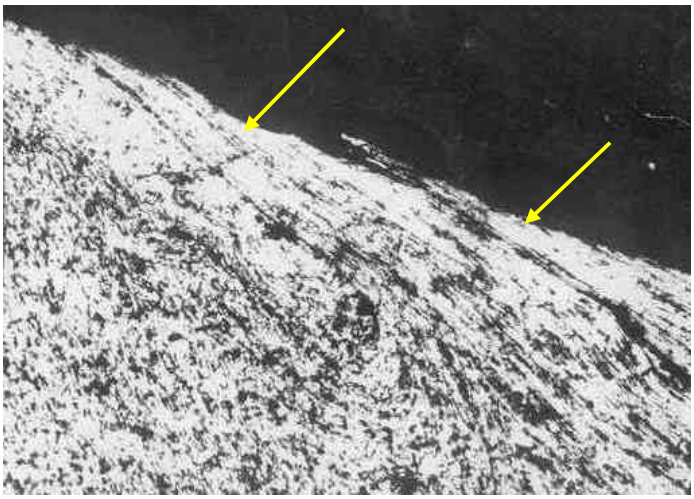

x160

Fig. 21 White layer in the UIT zone

The UIT process is accompanied by quick local heating of material in the ultrasonic impact point and quick heat removal from the area. In addition, intense plastic deformation occurs in this area. The combination of the above conditions produces the material with new properties that appears on metallographic pictures as a "white layer" [6, 9], which is not apt to etching. This material has no structure and is characterized by high contact strength and corrosion resistance. The portion of the white layer obtained on the initial material 10Mn2VBe is shown in Fig. 21.

Thus, the experimental studies presented in this section made it possible to establish that UIT is accompanied by the deformation resistance reduction, material structure modification and relaxation activation under ultrasonic vibrations and ultrasonic stress waves initiated by the ultrasonic impact. This results in higher efficiency of plastic deformations; reduction in unfavorable tensile stresses, e.g., in welded joints; replacement of tensile stresses by favorable compressive stresses; specified (directed) modification of the material condition and properties. UIT can be widely used in industry because of a simple contact action upon the surface and simple introduction of high-intensity ultrasound in the material by means of the ultrasonic impact.

5. IMPACT ADJUSTMENT AND TREATMENT QUALITY CONTROL

As referenced above, one of fundamental difference of ***Esonix*** UIT is the impulse excitation of ultrasonic impacts. This makes it possible to optimize the relation between the time of the impact action upon the object and the time of ultrasonic transducer operation, to continuously (at millisecond increments) obtain the information about the process of action upon the treatment

object through the back magnetostriction signal during a pause between impulses/impacts, to continuously inspect the condition of the treated material and provide in-process control of the treatment process in real time, as well as to control this process based on the continuous information [9]. Oscilloscope pictures of the impact under continuous and pulse excitation of the transducer are shown in Figs. 22 and 23 respectively. The top diagrams (magenta color) represent the transducer excitation signals, while the bottom diagrams (yellow color) represent the impact initiated by transducer vibrations. The comparison of the oscilloscope pictures shows the fundamental difference between impacts under different excitation conditions (continuous and pulse).

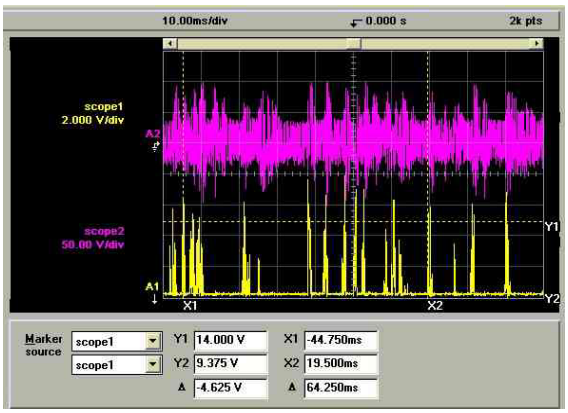

Fig. 22 Oscilloscope picture of impacts under continuous excitation of transducer

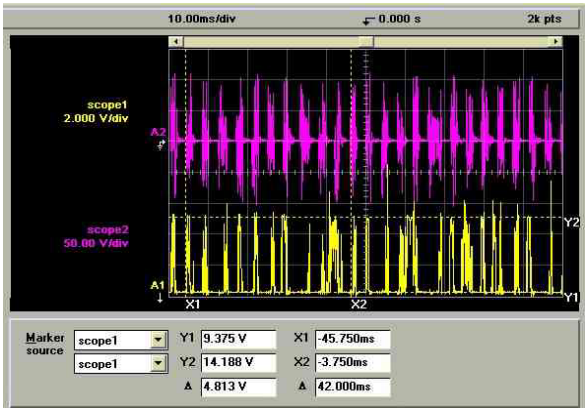

Fig. 23 Oscilloscope picture of impacts under pulse excitation of transducer

It should be noted that in the case of continuous excitation of the transducer the pause is not the source of the information necessary to control the treatment process, because the stochastic periods, wherein it exists, are filled with non-productive idle drive signal sent from the generator to the transducer, while under pulse excitation conditions the pause between impulses is used to record and analyze natural vibrations of the transducer, which is performed under loaded conditions as well, as shown in Figs. 24 and 25.

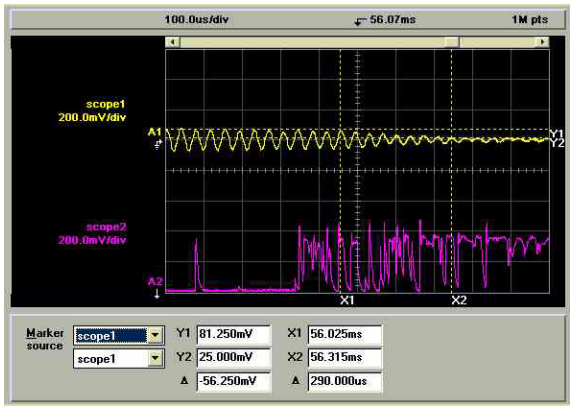

Fig. 24 Damping of transducer natural vibrations at the beginning of treatment

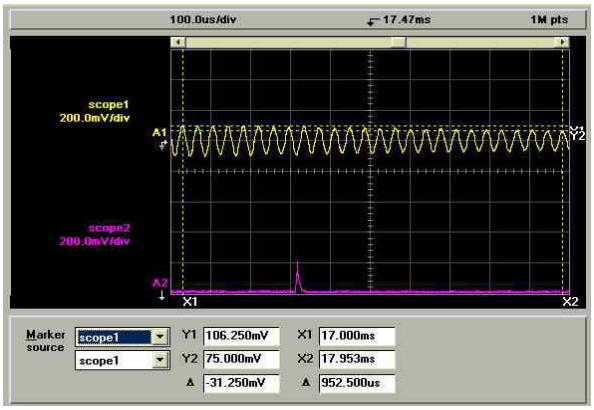

Fig. 25 The change in damping of transducer natural vibrations during treatment

It can be seen that as the treated material is saturated with ultrasonically induced plastic deformations, the absorption of the ultrasonic impact energy is reduced, while the amplitude of transducer natural vibrations in pause is increased. Since these parameters are constantly recorded, this provides a possibility to evaluate, at each instant of time, the extent of changes

made to the material condition, and to make a control decision (manual or automated) on treatment termination in a given area as these parameters stabilize. Note that for each specified technical effect of UIT there is an experimentally found or design impact energy level, which is determined by a specified and controlled (with accuracy of up to 1 μm) vibrational amplitude of loaded transducer, ultrasonic impact frequency and equivalent mass in the impact point, as described in [8].

As an example of the implementation of the UIT quality control in practice we provide micrographs, showing the steel mesostructure obtained under continuous and pulse excitation of transducers, see Figs. 26 and 27.

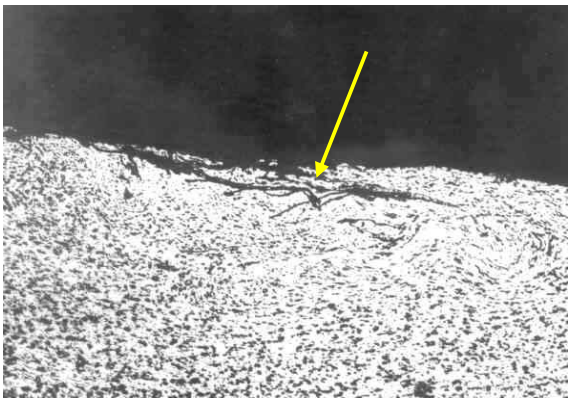

Fig. 26 Mesodefect in the center of a groove caused by local metal overstrengthening under condition of random impacts initiated by continuous excitation of the transducer (x160)

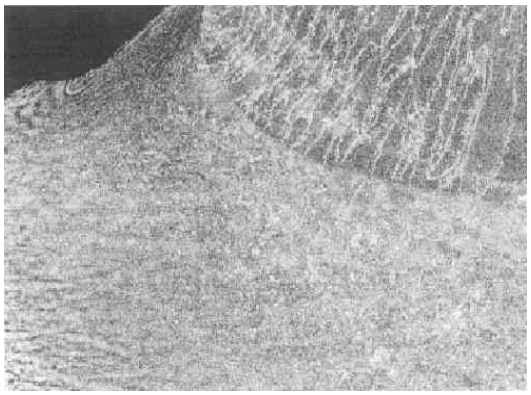

Fig. 27 Mesostructure of a groove formed under pulse excitation of the transducer with surface quality control per the UIT *Esonix* technology (x160)

6. UIT EQUIPMENT

The approaches described above made possible the gamut of UIT equipment for application in the field conditions (hand tool), continuous manufacture together with PLC and robots, manufacture of machine components and in production lines together with the mechanized devices. Examples of the industrial equipment designed to support the ***Esonix*** UIT are shown below in Figs. 28-34.

Fig. 28 UIT *Esonix* system with manual tool

Fig. 29 PLC *Esonix* unit

Fig. 30 Mechanized UIT of welds

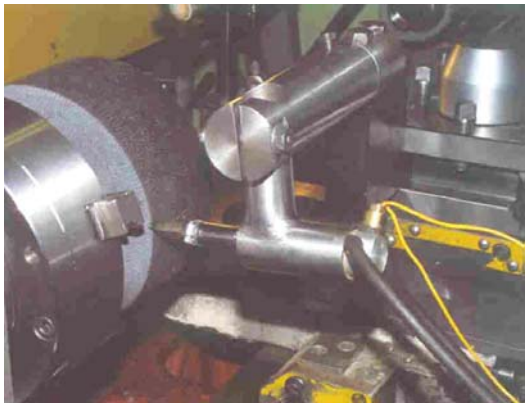

Fig. 31 UIT on a lathe

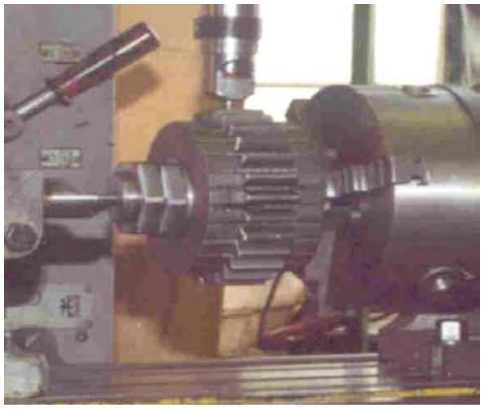

Fig. 32 UIT on a milling machine

Fig. 33 Range of high-power hand tools

Fig. 34 Tool for UIT *Esonix* on machines and robots

At this point, I will restrict myself to a short description of the developments we made, since UIT tool performance, which is responsible for the technical requirements of the entire process system, will be presented in more detail in document XIII-2005-04.

Esonix equipment can be used in any industrial and climatic conditions, in the atmosphere and aggressive environments, under water, in stationary industrial systems and in the field, during processing materials and joints of any strength to comply with the productivity, economic and safety requirements set by the customer.

7. CONCLUSIONS

1. In the process of UIT, the ultrasonic impact is the main carrier of the technical effect.

2. The main parameters of the ultrasonic impact efficiency include the duration of the ultrasonic impact and the frequency spectrum of indenter ultrasonic vibrations.

3. The ultrasonic impact generates ultrasonic impulses and ultrasonic stress waves in the material being treated.

4. Impulses initiated by the ultrasonic impact and ultrasonic stress waves reduce the material resistance to deformations and stresses induced during prior manufacturing process and during impact.

5. The ultrasonic impact is accompanied by quick local heating up to phase transformation temperatures and quick heat removal from the contact area, as well as plastic deformation due to impact.

6. Impulse thermo-acoustic-mechanical effects upon the workpiece in the ultrasonic area effectively modify the properties, condition and characteristics of the material in the UIT area.

7. The impulse excitation of the transducer and the initiating of the ultrasonic impact define the basic design principles for UIT processes, equipment and control systems.

REFERENCES

1. Mukhanov, I.I., Yu.M. Golubev, Strengthening Steel Components by Ultrasonically Vibrating Ball (in Russian), Vestn. Mashin., No. 11, p. 52, 1966.

2. Mordvintseva, A.V., Ultrasonic Treatment of Welded Joints (in Russian), in: Ultrasonic Applications in Welding Engineering, Moscow, TsINTIEnergomash, Proc. of N.E. Bauman MVTU, ed. 35, 1959.

3. Krylov, N.A., A.M. Polischuk, The Use of Ultrasonic Equipment for Metal Structure Stabilization (in Russian), In: Basic Physics of Industrial Ultrasonic Applications, Part 1, LDNTP, p. 70, 1970.

4. Statnikov, E.Sh., L.V. Zhuravlev, A.F. Alekseev et al., Ultrasonic Head for Strain Hardening and Relaxation Treatment (in Russian), USSR Inventor's Certificate No. 472782, Published in Byull. Izobret., No. 21 (1975).

5. Prokopenko, G.I., V.P. Krivko, Ultrasonic Multiple-striker Tool (In Russian), USSR Inventor's Certificate No. 601043, Published in Byull. Izobret. (1978).

6. Statnikov, E.S, Ultrasonic Impact Methods for Treatment of Welded Structures, US Patent 6, 171, 415 B1 (2001).

7. Statnikov, E.S., Means and Method for Electroacoustic Transducer Excitation, US Patent 6,289,736 B1 (2001).

8. Statnikov, E.S., Ultrasonic Machining and Reconfiguration of Braking Surfaces, US Patent 6,458,225 (2002).

9. Statnikov, E.S., Ultrasonic Impact Methods for Treatment of Welded Structures, US Patent 6,338, 765 (2002).

10. Statnikov, E.S., Ultrasonic Machining and Reconfiguration of Braking Surfaces, US Patent 6,722,175 (2004).

11. Statnikov, E.S., Ultrasonic Impact Methods for Treatment of Welded Structures, US Patent Application 10/015,670.

12. Statnikov, E.S., Ultrasonic Impact Machining of Body Surfaces to Correct Defects & Strengthen Work Surfaces, US Patent Application 10/207, 859.

13. Statnikov, E.S., Ultrasonic Impact Machining of Body Surfaces to Correct Defects & Strengthen Work Surfaces, PCT Application PCT/US03/11791

14. Statnikov, E.S., Applications of Operational Ultrasonic Impact Treatment (UIT) Technologies in Production of Welded Joints, IIW, Doc. XIII-1667-97.

15. Statnikov, E.S, Guide for Application of Ultrasonic Impact Treatment for Improving Fatigue Life of Welded Structures, IIW, Doc. XIII-1757-99.

16. Statnikov, E.S., V.O. Muktepavel, A. Blomqvist, Comparison of Ultrasonic Impact Treatment (UIT) and other Fatigue Life Improvement Methods, IIW, Doc. XIII-1817-00.

17. Galtier, A., E.S. Statnikov, The Influence of Ultrasonic Impact Treatment on Fatigue Behaviour of Welded Joints in High-Strength Steel, IIW, Doc. XIII-1976-03.

18. Haagensen, P.J., E.S. Statnikov, Louis Lopez-Martinez, Introductory Fatigue Tests on Welded Joints in High Strength Steel and Aluminium Improved by Various Methods Including Ultrasonic Impact Treatment (UIT), IIW, Doc. XIII-1748-98.

19. Fisher, J.W., E.Sh. Statnikov, L. Tehini, Fatigue Strength Enhancement by Means of Weld Design Change and the Application of Ultrasonic Impact treatment, Proc. of Intl. Symp. on Steel Bridges, Chicago (2001).

20. Lihavainen, V.M., G. Marquis, E.S. Statnikov, Fatigue Strength of a Longitudinal Attachment Improved by Ultrasonic Impact Treatment, IIW Doc. XIII-1990-03.

21. Statnikov, E.Sh., V.O.Muktepavel, V.N.Vityazev, V.I.Trufyakov, V.S.Kovalchuk and P.Haagensen, Comparison of the Improvement in Corrosion Fatigue Strength of Weld Repaired Marine Cu 3-grade Bronze Propellers by Ultrasonic Impact Treatment (UIT) or Heat Treatment, IIW Doc. XIII-1964-03.

22. Janosch, J.J., H. Koneczny, S. Debiez, E.Sh. Statnikov, V.I. Trufyakov, P.P. Mikheev, Improvement of Fatigue Strength in Welded Joint (in HSS and Aluminium Alloy) by Ultrasonic Hammer Peening, IIW Doc. XIII-1594-95.

23. Statnikov, E.Sh., V.N. Vityazev, O.V. Korolkov, Study of Comparative Characteristics of Ultrasonic Impact and Optimization of Deformation Treatment Processes, 5th World Congress on Ultrasonics, Paris, France (2003)

24. Haagensen, P.J., Weld Improvement Methods – Applications and Implementations in Design Codes, invited paper at the Conference on Fatigue of Welded Structures, Senlis, Paris, France, 12-14 June, 1996.

25. Prokopenko, G.I., T.A. Lyatun, Study of Surface Hardening Conditions by Means of Ultrasound, in: Physics and Chemistry of Material Processing, No. 3, p 91, 1977.

26. Blaha, F., B.Langenecker."Dehnung von Zink-Kristallen unter Ultraschalleinwirkung", Zeitschrift die Naturwissenschaften, 20, 556, 1955.

27. Konovalov, E.G., V.M. Drozdov, M.D. Tyavlovski, Dynamic Strength of Metals (in Russian), Nauka i Tekhnika, Minsk, 1969.

28. Kazantsev, V.F., Basic Physics of Ultrasonic Action on Solid Body Processing (in Russian). Doctoral thesis, AKIN, Moscow, 1980, pp.12-44.

29. Statnikov, E.Sh., L.O. Makarov, Yu.P. Kozlov, Method of Optimizing Magnetostrictive Electroacoustic Transducers (in Russian), USSR Inventor's Certificate No. 300224, Published in Byull. Izobret., No. 13 (1976).

30. Statnikov, E.S., Development and Study of Ultrasonic Specific-purpose Devices, Thesis, Academician N.N. Andreyev Acoustic Institute, Academy of Sciences of the USSR, 1982.

31. Severdenko, V.P., E.G. Konovalov, E.Sh. Statnikov et al., Study of Mechanical Properties of New Materials under Ultrasonic Oscillations, Report # 21-971, FTI Acad. Nauk of BSSR, Minsk (1966).

32. Statnikov, E.Sh., Activation of Deformation Process under Ultrasonic Effect,. Scientific and Technical Conference “XXX Lomonosov Readings”, Sevmashvtuz, Severodvinsk (2001).